

# Effect of potentiostatic waveforms on properties of electrodeposited NiFe alloy films

H. Kockar<sup>1,a</sup>, M. Alper<sup>2</sup>, and H. Topcu<sup>1</sup>

<sup>1</sup> Physics Department, Science and Literature Faculty, Balikesir University, 10100 Balikesir, Turkey

<sup>2</sup> Physics Department, Science and Literature Faculty, Uludag University, Görükle, 16059 Bursa, Turkey

Received 30 March 2004

Published online 18 January 2005 – © EDP Sciences, Società Italiana di Fisica, Springer-Verlag 2004

**Abstract.** The influence of the deposition potentials applied in continuous and pulse waveforms on the properties of the electrodeposited NiFe alloy films have been investigated. The films were grown on (100) textured polycrystalline copper substrates. During growth, the films were characterized by recording the current-time transients. The composition of samples was determined by inductively coupled plasma atomic emission spectrometry (ICP-AES). The analysis results revealed that the Fe content in the films decreases as both the deposition potential and the film thickness increase. The X-ray patterns showed that the films have face centred cubic (fcc) structure as their substrates and the (111) texture. The magnetic characteristics of films studied by a vibrating sample magnetometer (VSM) were found to vary depending on the type of the deposition (pulse or continuous) and the thickness of samples. The easy axis is in the film plane for all samples.

**PACS.** 81.15.Pq Electrodeposition, electroplating – 81.07.Bc Nanocrystalline materials – 75.70.Ak Magnetic properties of monolayers and thin films

## 1 Introduction

Electrodeposited magnetic thin films such as NiFe, CoFe and NiCoFe have become the subject of intense investigations since they have both beneficial magnetic properties at room temperature [1] and exhibit the anomalous codeposition behaviour [2,3]. In particular, the permalloy films consisting of 80% Ni and 20% Fe are widely used in the industrial applications such as magnetic recording and storage devices. In addition to their technological applications, these films are also scientifically of considerable importance due to the anomalous codeposition. In the electrodeposition of NiFe, the less noble metal Fe deposits preferentially; that is, its content in the deposit is much higher compared to the more noble metal Ni, even though its concentration in the solution is lower. Therefore, a large effort has been spent to investigate the anomalous codeposition and magnetic properties of electrodeposited NiFe films [4–6].

The structural and magnetic properties of electrodeposited NiFe films are mainly dictated by a number of factors including the deposition potentials, the electrolyte pH and temperature, the current density, the concentration of metal ions to be deposited. In addition to these parameters, the presence of additives or impurities and whether the current is pulsed or continuous are also impor-

tant variables in the electrodeposition [7–10]. Therefore, the deposition parameters may need to be varied to obtain high quality films in the electrodeposition of metal and alloys. Some studies showed that the current waveforms affect the structural, magnetic, and mechanical characteristics of deposits [11,12].

In this work, a series of NiFe alloy films have been grown on (100) textured polycrystalline Cu substrates using three different cathode potentials applied in continuous and pulse waveforms. It was investigated how the structural and magnetic properties of these films have been affected by the applied potential waveforms. Furthermore, the effect of the film thickness on the properties has been studied for the cathode potential kept constant at  $-1.5$  V with respect to the saturated calomel electrode (SCE).

## 2 Experimental

The NiFe films were electrodeposited on (100) textured polycrystalline Cu sheets using a cell with three electrodes under potentiostatic conditions. Prior to the deposition, one face of the Cu substrates were first polished with emery paper and then covered by electroplating tape, except for an area of  $\sim 3$  cm<sup>2</sup>. The uncovered area, which is exposed to the electrolyte, was electropolished with 50% orthophosphoric acid. The polished Cu substrates

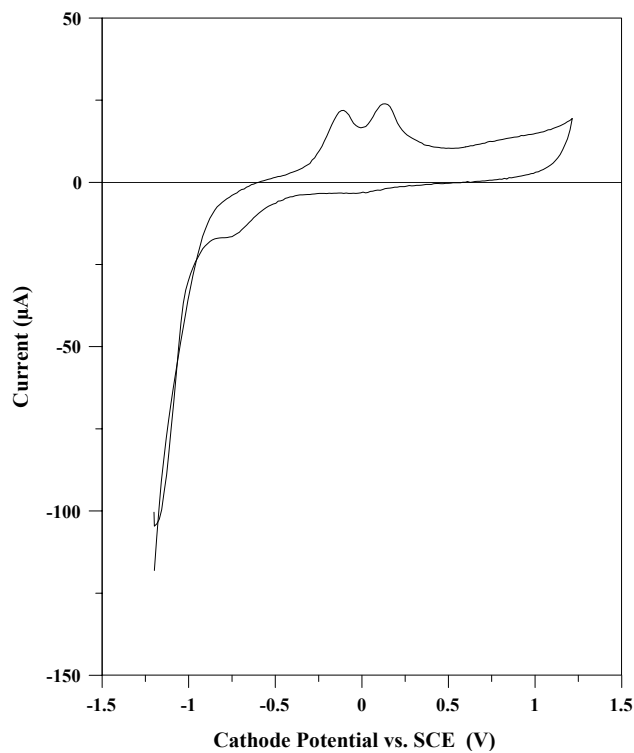
<sup>a</sup> e-mail: hkockar@balikesir.edu.tr

were used as cathodes, whereas the anode a platinum foil of  $6 \text{ cm}^2$ . The reference electrode was a saturated calomel electrode (SCE). All potentials were referred to the SCE. The plating electrolyte was prepared by dissolving reagent grade chemicals in distilled water. The electrolyte composition consisted of  $0.05 \text{ M NiSO}_4 \cdot 7\text{H}_2\text{O}$ ,  $0.01 \text{ M FeSO}_4 \cdot 7\text{H}_2\text{O}$  and  $0.1 \text{ M H}_3\text{BO}_3$ . All electrochemical experiments were carried out at room temperature using an EGG Potentiostat/Galvanostat (Model 362) interfaced with a personal computer (PC) with our own software. The films were deposited at the cathodic potentials of  $1.2 \text{ V}$ ,  $1.5 \text{ V}$  and  $1.8 \text{ V}$  vs. SCE, which were applied in both continuous and pulse waveforms. In the pulse plating, the deposition potentials were stepped from the selected potential value to  $-0.8 \text{ V}$  vs. SCE. At the selected potential values ( $-1.2 \text{ V}$ ,  $-1.5 \text{ V}$  and  $-1.8 \text{ V}$ ), a NiFe layer thickness of  $5 \text{ nm}$  was deposited while at  $-0.8 \text{ V}$  a layer of  $0.1 \text{ nm}$ . This process was continued until the desired total thickness reached. For these series of samples, the total film thickness was fixed at  $2 \mu\text{m}$ . Furthermore, the films with different thickness were also produced by keeping constant the cathode potential at  $-1.5 \text{ V}$  vs. the SCE. The charge amounts required for the desired film thicknesses were calculated according to the Faraday Law by assuming 100% current efficiency.

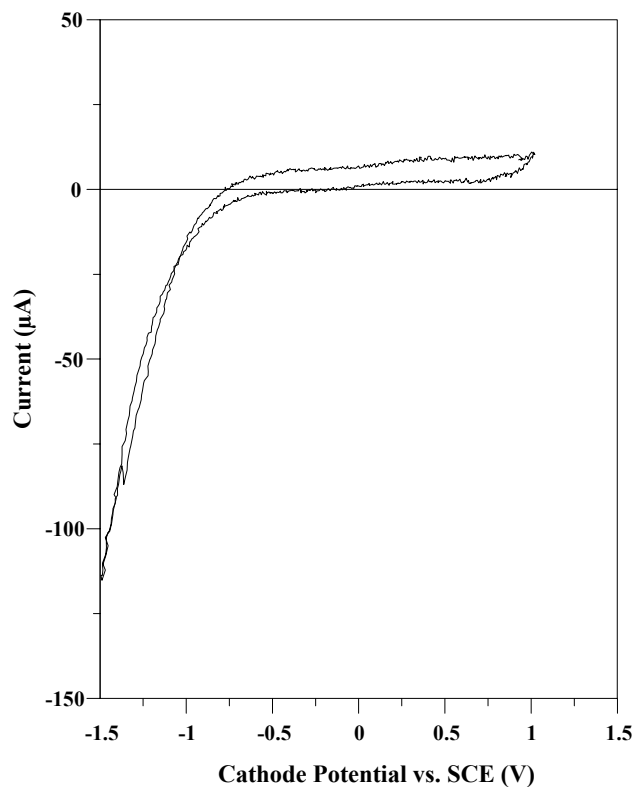
The electrolyte characterisations were studied using the cyclic voltammetry method with a potential scan rate of  $200 \text{ mV/s}$ . The scans were performed on a Pt wire electrode with an area of  $\sim 0.02 \text{ cm}^2$  in the cathodic direction (from  $+1.0 \text{ V}$  to  $-1.2 \text{ V}$  vs. SCE). The growth mechanisms of NiFe films were studied by recording the current-time transients during deposition. The structural analysis of the deposits on the Cu substrates was made using a Philips X-ray diffractometer (PW1820) with a  $\text{Cu K}\alpha$  radiation. The magnetic properties were investigated with a vibrating sample magnetometer (VSM, Moltspin Ltd.). After growth, the films were stripped from their Cu substrates electrochemically using a chromic acid solution to make the compositional analysis. The composition of the films was determined by an inductively coupled plasma atomic emission spectrometry, (ICP-AES). The deposits were first solved in an acid mixture and then diluted. The spectrometer, a Perkin Elmer Optima 3100 XL, was calibrated with standard solutions prepared from commercial reference solutions (Titrisol, Merck). The analytical wavelengths for Ni and Fe were  $231.6 \text{ nm}$  and  $238.2 \text{ nm}$  respectively.

### 3 Results and discussion

The cyclic voltammetry (CV) technique was used to estimate the deposition potential for NiFe alloy and study the characterizations of Ni and Fe deposition process. Figure 1a shows the cyclic voltammetry curve of the solution used to deposit NiFe alloy films. As seen from the CV curve in Figure 1a, there is no considerable current flowing in the potential region between  $+0.3 \text{ V}$  and  $-0.5 \text{ V}$ . The metal deposition is observed to start at around  $-0.5 \text{ V}$  vs. SCE. As the cathode potential increases



(a)



(b)

**Fig. 1.** (a) Cyclic voltammetry for the solution ( $0.05 \text{ M NiSO}_4 \cdot 7\text{H}_2\text{O}$ ,  $0.01 \text{ M FeSO}_4 \cdot 7\text{H}_2\text{O}$  and  $0.1 \text{ M H}_3\text{BO}_3$ .) used to deposit NiFe films. (b) Cyclic voltammetry for a solution containing  $0.05 \text{ M NiSO}_4 \cdot 7\text{H}_2\text{O}$  and  $0.1 \text{ M H}_3\text{BO}_3$ .

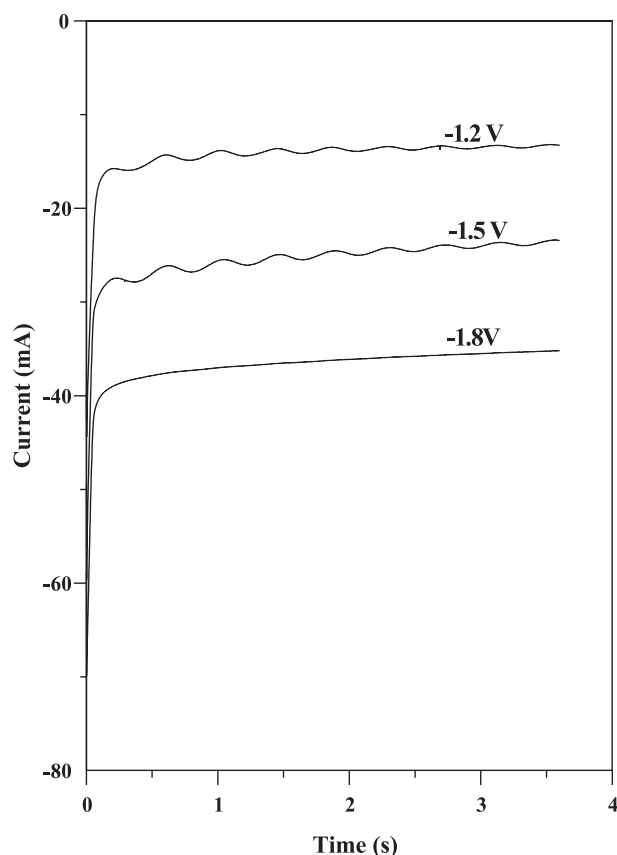


**Fig. 2.** Current-time transients for NiFe films deposited at different cathode potentials in continuous current waveform.

from  $-0.5$  V, the current also increases and reaches a peak value at  $-0.7$  V. This peak probably corresponds to the reduction of  $\text{Fe}^{2+}$  and/or  $\text{Fe}^{3+}$  ions, because the Ni deposition does not occur at the more positive potentials below  $-0.8$ , as seen in Figure 1b, which is the CV curve of the solution containing only  $0.05$  M  $\text{NiSO}_4 \cdot 7\text{H}_2\text{O}$  and  $0.1$  M  $\text{H}_3\text{BO}_3$ , but not  $\text{FeSO}_4 \cdot 7\text{H}_2\text{O}$ . When the electrolyte is void of iron, the current almost remains zero until the onset of Ni deposition ( $-0.8$  V) is achieved. Also as seen in Figure 1a, significant metal deposition commences at about  $-0.8$  V for the electrolyte with Fe. The cathodic current steeply increases with increasing potential, due to the deposition of both Ni and Fe ions in the electrolyte. When the potential is reversed the current follows the same potential dependence back to  $-0.8$  V. After the potential reaches at  $-0.6$  V, an anodic current starts to flow. On the anodic side, two separate peaks are seen; one at  $-0.2$  V and other at  $+0.2$  V. These peaks are probably due to the dissolution of Fe, because as seen in the CV curve of the solution containing only Ni (without Fe) in Figure 1b, the Ni dissolution does not occur in the potential regions on the anodic side. This result agrees with previous work [2]. Based on the results obtained from the CV curves, a potential region between  $-0.8$  V and  $-1.8$  V vs. SCE was selected for the deposition of NiFe alloys.

The current was recorded as a function of time to study the deposition mechanisms of NiFe alloys during growth.

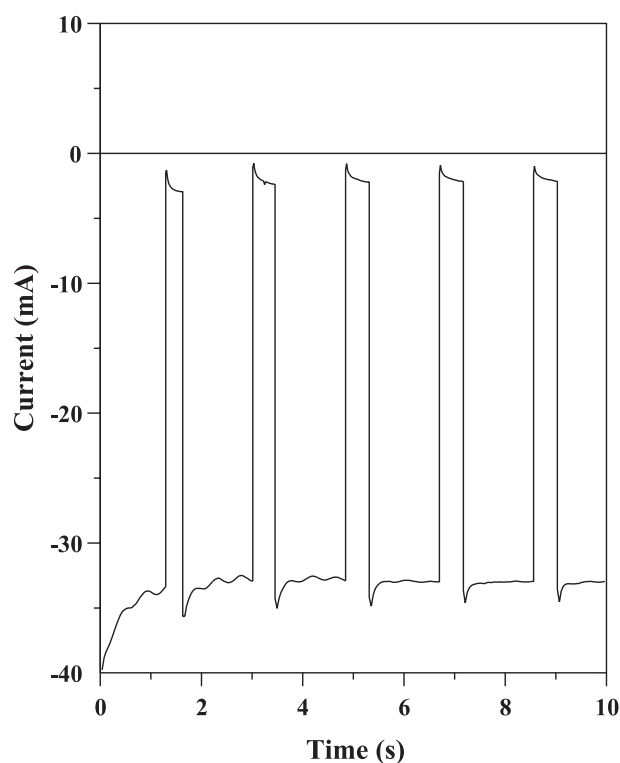


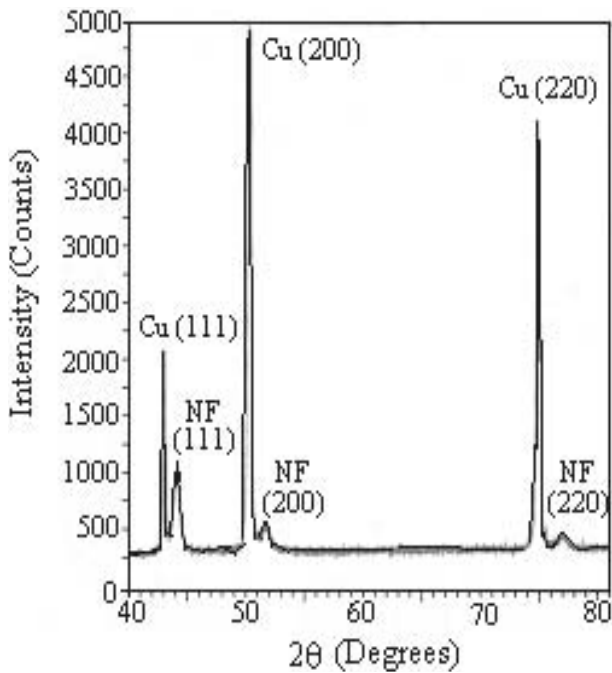
**Fig. 3.** Current-time transients for the cathode potentials stepped from  $-1.8$  V to  $-0.8$  V vs. SCE during growth of a NiFe film.

The current-time transient curves for three different potentials ( $-1.2$  V,  $-1.5$  V and  $-1.8$  V vs. SCE) applied in continuous current waveforms are shown in Figure 2. As seen from the figure, at the beginning of the applied potentials, a high cathodic current is seen for a short time. Then, the current rapidly decreases, due to the depletion of the metal ion concentrations close to the electrode surface, and subsequently reaches a stable value. As the cathode potential is increased the current also increases. In the case of pulse plating, Figure 3 shows the current-time transients for the cathode potentials stepped from  $-1.8$  V to  $-0.8$  V. The high negative current pulses correspond to the NiFe layers with the thickness of  $5$  nm, while the low current pulses to the NiFe layers with a thickness of  $1$  nm. It was observed that the current increases as the cathode potential increases, as in the continuous plating. Similar curves were also obtained for the potentials stepped from  $-1.5$  V to  $-0.8$  V and  $-1.2$  V to  $-0.8$  V. The average current densities for the potentials applied in both continuous and pulse waveforms were found to be in agreement with each other, see also Table 1.

The crystalline structure and texture of NiFe alloy films on their Cu substrates were examined using X-ray diffraction in the range of  $40^\circ < 2\theta < 80^\circ$ . As an example, the XRD pattern of a NiFe film with  $2$   $\mu\text{m}$  thickness, which was deposited at  $-1.5$  V in continuous waveform, is shown in Figure 4. In the figure, the peaks labelled as NF(111), NF(200) and NF(220) correspond to the main Bragg reflections for (111), (200) and (220) planes,

**Table 1.** The elemental and magnetic measurement results for NiFe films deposited at different potentials and with different thickness.

Type of deposition potential	Thickness of the films ( $\mu\text{m}$ )	Cathode potential vs. the SCE (V)	Current density ( $\text{mA}/\text{cm}^2$ )	Composition Analysis		Magnetic analysis	
				% Ni	% Fe	$M_o$ (kA/m)	$H_c$ (kA/m)
Continuous	2	-1.2	3.53	69.56	30.43	523	0.5
	2	-1.5	6.20	79.72	20.28	462	0.6
	2	-1.8	9.36	87.98	12.01	437	0.9
Pulse	2	-1.2	3.34	71.74	28.26	509	0.7
	2	-1.5	6.69	80.03	19.97	485	0.8
	2	-1.8	8.92	87.81	12.19	477	1.1
Continuous	1	-1.5	6.69	76.44	23.56	539	0.4
	2	-1.5	6.53	79.72	20.28	462	0.6
	3	-1.5	6.53	82.85	17.15	443	1.0

**Fig. 4.** XRD pattern of the NiFe film deposited at  $-1.5$  V vs. SCE in continuous waveform.

respectively, of NiFe alloy. The peaks of the Cu substrate were marked to be Cu(111), Cu(200) and Cu(220), which indicates the reflections from the (111), (200) and (220) planes of the face-centered cubic (fcc) structure, respectively. We can conclude that the NiFe alloy film has the same crystal structure (fcc) as its substrate. However, the strongest peak in the pattern of the film is the (111) reflection, whereas the strongest peak of the substrate is the (200). This indicates that the NiFe film textured preferentially in the (111) direction. The interplanar spacings,  $d_{(hkl)}$ , were calculated to be 0.2083 nm, 0.1761 nm and 0.1251 nm from the positions of NF(111), NF(200)

and NF(220) peaks, respectively. Similar results were also found for other NiFe films deposited at different potentials in both continuous and pulse waveforms. In all samples, no reflection of Fe in body-centered cubic (bcc) structure was observed, although single electrodeposited Fe films exhibited bcc phase [11]. This arises probably from the low concentration of the Fe content in the deposits. The elemental analysis results confirmed that the Fe content in our films has remained below 31% wt. (see Tab. 1). Previous studies [1,5,13,14] showed that the electrodeposited NiFe films having such low Fe contents have always fcc structure.

The elemental analysis of the NiFe deposits obtained from the ICP-AES measurements is shown in Table 1. The measurements indicate that the Fe content of NiFe films with  $2 \mu\text{m}$  thickness decreases as the cathode potential applied in both continuous and pulse waveforms increases. The Fe contents of the continuous wave films are in good agreement with those of the pulse wave film. As seen from Table 1, the anomalous codeposition of Fe is observed only for the films deposited at  $-1.2$  V. For the films produced at  $-1.5$  V, the ratio of Ni to Fe is almost the same as that in the electrolyte. The Ni ratio in the films grown at  $-1.8$  V is higher than that in the electrolyte. On the other hand, for the films with different thickness prepared at a constant cathode potential ( $-1.5$  V), the Fe content decreases as the film thickness is increased. The decrease of the Fe content with both increasing potential and thickness may be due to the depletion of Fe ion concentrations in a short time, since the Fe concentration in the electrolyte is very low.

The magnetisations of NiFe films were measured at room temperature using a vibrating sample magnetometer (VSM). A magnetic field of up to 800 kA/m was applied both parallel and perpendicular to the plane of the film. As an example, the hysteresis curve of a NiFe film with  $2 \mu\text{m}$  thickness, which was deposited at  $-1.5$  V in continuous waveform, is shown in Figure 5.

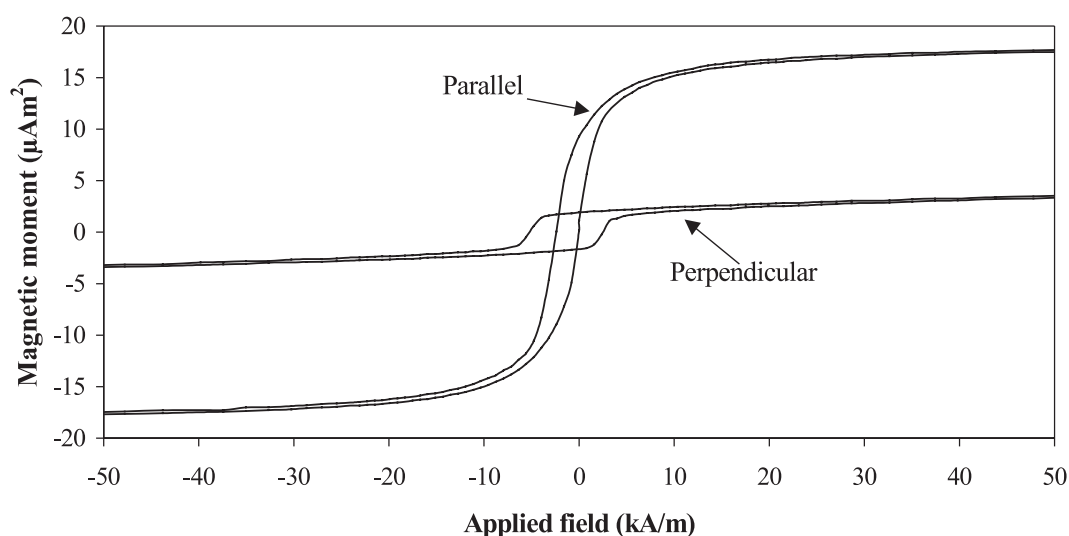


Fig. 5. Hysteresis loops for the NiFe film deposited at  $-1.5$  V vs. SCE in continuous waveform.

As can be seen in Figure 5, the in-plane hysteresis loop shows a higher remanent magnetisation and lower saturation field than the perpendicular hysteresis loop. This indicates that the easy axis direction of the magnetisation is parallel to the film plane and the hard axis of hysteresis loop is perpendicular to the film plane. As a result of demagnetising effect, the film shape anisotropy dictates that the specimen must have planar easy axis. It was found that all samples have similar planar magnetisation loops. For all films, the magnetisations and coercivities are summarised in Table 1. As seen from Table 1, as the Fe content of the films decreases, the coercivity increases and the magnetisation decreases. Furthermore, similar results were also found for the thicker samples. This may be due to the decrease of the Fe content in the deposit.

#### 4 Summary

The ferromagnetic NiFe alloy films were electrodeposited on (100) textured polycrystalline copper substrates at the cathode potential applied in continuous and pulse waveforms. It was found that the films exhibited fcc crystalline structure and grew preferentially in the (111) direction. The elemental analysis results showed that the Fe content of films decreases with increasing the potential and the thickness. The magnetic properties were observed to vary depending on the type of deposition and the thickness of the samples, and also all films have planar magnetisation.

This work is supported by the Scientific and Technical Research Council (TUBITAK) of Turkey under Grant no. TBAG-1771, and Balikesir University, Turkey under Grant no. 2001/02. The authors are grateful to Dr. T. Meydan

for the use of the XRD and VSM at Wolfson Centre, Cardiff University, UK and to Dr. N. Nakiboglu for his help in the ICP-AES measurements at Research Centre of Applied Sciences (BURCAS), Balikesir University, Turkey.

#### References

1. N.V. Myung, K. Nobe, *J. Electrochem. Soc.* **148** (3), C136 (2001)
2. D. Gangasingh, J.B. Talbot, *J. Electrochem. Soc.* **138** (12), 3605 (1991)
3. Y. Zhuang, E.J. Podlaha, *J. Electrochem. Soc.* **150** (4), C219 (2003)
4. W.C. Grande, J.B. Talbot, *J. Electrochem. Soc.* **140** (3), 669 (1993)
5. S.D. Leith, S. Ramli, T. Schwartz, *J. Electrochem. Soc.* **146** (4), 1431 (1999)
6. T.M. Harris, J.L. Wilson, M. Bleakley, *J. Electrochem. Soc.* **146** (4), 1461 (1999)
7. V.C. Kieling, *Surf. Coat. Technol.* **96**, 135 (1997)
8. J. Horkans, *J. Electrochem. Soc.* **128** (1), 45 (1981)
9. A. Afshar, A.G. Dolati, M. Ghorbani, *Mater. Chem. Phys.* **77**, 352 (2002)
10. K.-M. Yin, B.-T. Lin, *Surf. Coat. Technol.* **78**, 205 (1996)
11. D.L. Grimmer, M. Schwartz, K. Nobe, *J. Electrochem. Soc.* **140** (4), 973 (1993)
12. D.L. Grimmer, M. Schwartz, K. Nobe, *J. Electrochem. Soc.* **137** (11), 3414 (1990)
13. M. Saitou, W. Oshikawa, M. Mori, A. Makabe, *J. Electrochem. Soc.* **148**, C780 (2001)
14. X. Liu, P. Evans, G. Zangari, *J. Magn. Magn. Mater.* **226-230**, 2073 (2001)